ACS APPLIED MATERIALS & INTERFACES

Research Article

www.acsami.org

pH-Dependent Synthesis of Novel Structure-Controllable Polymer-Carbon NanoDots with High Acidophilic Luminescence and Super Carbon Dots Assembly for White Light-Emitting Diodes

Siyu Lu,[†,§] Ridong Cong,[∥] Shoujun Zhu,[†,⊥] Xiaohuan Zhao,[†] Junjun Liu,[†] John S.Tse,[⊗,§] Sheng Meng,[‡] and Bai Yang*[,†]

[†]State Key Laboratory of Supramolecular Structure and Materials, College of Chemistry and [⊗]State Key Laboratory of Suprhard Materials, Jilin University, Changchun 130012, P. R. China

[‡]Beijing National Laboratory for Condensed Matter Physics, and Institute of Physics, Chinese Academy of Sciences, 100190 Beijing, China

[§]Department of Physics and Engineering Physics, University of Saskatchewan, Saskatoon, Saskatchewan S7N 5E2, Canada

[⊥]Department of chemistry, Stanford University, Stanford, California 94305, United States

[∥]Hebei Key Laboratory of Optic Electronic Information Materials, College of Physics Science and Technology, Hebei University, Baoding 071002, P. R. China

Supporting Information

ABSTRACT: We use a pH-dependent solubility equilibrium to develop a one-pot aqueous synthesis of polymer carbon nanodots with novel structures. The chemical structure and photoluminescence (PL) were heavily influenced by the synthesis pH, with cross-linked polymer−carbon film (pH > 7), polymer carbon nanosheets (3 < pH < 7), and amorphous carbon structures (1 < pH < 3) achieved by altering the initial pH. Although pH-dependent structures frequently occur in typical semiconductors and supramolecular architectures involving metal, this is the first experimental work describing it in carbon nanodots. Supersmall carbon nanodots (SCNDs, ∼0.5 nm) were obtained at pH < 1; their direct white emission can be easily applied as an inexpensive color-changing layer in white LEDs. Investigation of the PL mechanism of the SCNDs revealed an uncommon multilevel highly emissive recombination channel, which could be possibly derived from the wide distributions of surface-state PL centers. Theoretical calculation of the single layer of the carbon dots further explored their band gap changes.

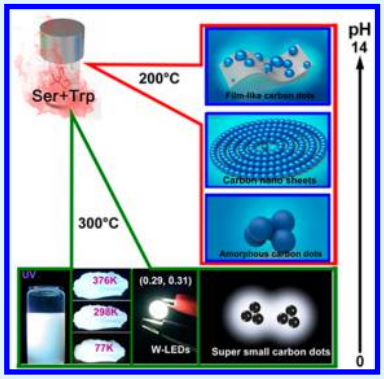

KEYWORDS: *carbon dots, structure controllable, molecular state, fluorophore, carbon core state*

INTRODUCTION

Throughout the history of fluorescent materials, considerable effort has been devoted to the development of heavy-metal-free and low-toxicity photoluminescence (PL) nanoprobes. Carbon nanodots (CNDs) are promising in this regard and have thus drawn much attention during the past decade.[1−4] They show high photostability without blinking,[5,6] and they have tunable emissions,[7] chemical inertness,[8] good biocompatibility,[9] and low toxicity.[10] They can be conveniently surface-modified and are cheaply produced.[11,12] We have previously reported that their quantum yield can be as high as 80%, which is comparable to even organic dyes.[13] Their strong properties make CNDs promising for use in applications such as biomedicine, optoelectronic devices, sensors, and assembly composites. Since the discovery of CNDs composed of a batch of single-wall nanotubes in 2004, thousands of starting materials and hundreds of approaches have been reported for their synthesis.[14−17] Reactants can vary from multicomponent chemical mixtures to natural products, while syntheses have been reported using laser ablation, pyrolysis, electrochemical oxidation, hydrothermal reactions, and microwave treatment, among others.[18,19] Although syntheses can vary greatly, the resulting CNDs are generally spherical, smaller than 10 nm, and present only blue PL that is quenched at low pH, thereby restricting their applicability.[20−25] Their chemical structure is generally closely related to their PL properties, and CNDs with novel structures sometimes show unique optical properties. Therefore, fabricating CNDs with novel structures is important to understand the PL mechanism and broaden their applicability. Herein, we report a new and facile route to synthesize four novel structures of polymer-CNDs (p-CNDs) by the hydrothermal process of two amino acids at different temperatures and pH values. The p-CNDs showed polymer chains coexisting with CNDs throughout the whole reaction, which represent a key factor for the formation of the novel structures. Changing the pH and temperature controlled the

Received: November 28, 2015
Accepted: January 21, 2016
Published: January 21, 2016

DOI: 10.1021/acsami.5b11579
ACS Appl. Mater. Interfaces 2016, 8, 4062−4068

product structures, with polymer−carbon film (p-CNDs-1), polymer−carbon nanosheets (p-CNDs-2), amorphous CNDs (p-CNDs-3), and supersmall CNDs (SCNDs) all possible. Although pH-dependent structures are frequently observed in typical semiconductors and supramolecular architectures involving metal, this is the first experimental report of them in CNDs.[26−28] The p-CNDs-1, p-CNDs-2, and p-CNDs-3 all emitted strong blue luminescence at high acidophilic condition, with the fluorescence intensity in acid at least twice that seen in a neutral solution. Therefore, these materials are able to detect H^+ sensitively and selectively. Additionally, the fluorescence of the three p-CNDs could also be quenched by Fe^{3+}. Unlike the CNDs, the SCNDs exhibited a strong white fluorescence, which can be used for direct white-light generation in white light-emitting diodes (LEDs). The PL mechanism of the SCNDs was also investigated through the theoretical calculation of their designed single layer.

RESULTS AND DISCUSSION

Synthesis and Characterization of Film Carbon Dots, Carbon Nanosheets, and Amorphous Nanoparticles. Our previous work used the one-step hydrothermal treatment of L-serine and L-tryptophan (molar ratio 3:1) in alkaline conditions (pH ≈ 8.1) at 200 °C to obtain p-CNDs-1.[29] The resulting carbon material comprised a large smooth film with embedded carbon dots, which were detectable by transmission electron microscopy (TEM) and high-resolution TEM (HR-TEM; Figure 2a). The material displayed extremely acidophilic high luminescence (61.12%). This promising novel structure led to the current work, an exploration of the relationship between the structure and PL emission of the p-CNDs. Aqueous L-serine and L-tryptophan were at different pH values (Figure 1), with all other conditions kept constant. Synthesis at

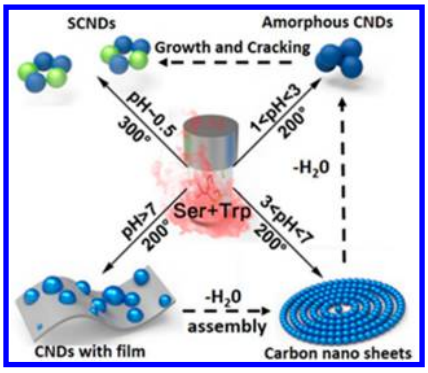

Figure 1. A schematic illustration of the preparation procedure of different structure carbon dots by hydrothermal carbonization of L-serine and L-tryptophan at different pH values and temperatures.

3 < pH < 7 generated regular layered structures (p-CND-2), with an average diameter of 50 nm (Figure 1c,d). At 1 < pH < 3, the reaction system produced p-CNDs-3 with an amorphous carbon core structure. The particles showed spherical symmetry and a relatively narrow size distribution, with an average diameter of ∼2 nm (Figure 2e,f). The optical properties of the above three samples were tested to uncover the influence of structure on PL (Figure 3). The UV−vis spectra of aqueous p-CNDs-1, p-CNDs-2, and p-CNDs-3 are shown in Figure 3a,c,e. The results for p-CNDs-1 showed the same peaks at 223 and 271 nm as previously reported, while p-CNDs-2 and p-CNDs-3 both showed peaks at 246 and 299 nm.

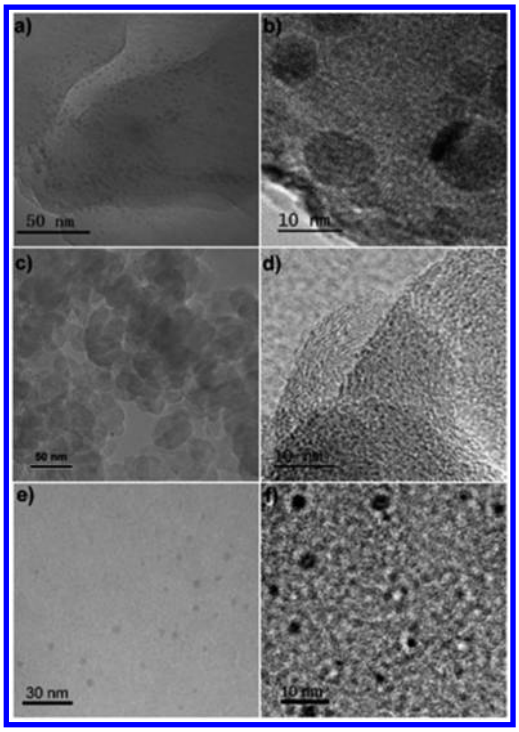

Figure 2. TEM and HR-TEM images of as-prepared (a, b) film-like carbon dots, (c, d) carbon nano sheets, and (e, f) amorphous carbon dots.

However, p-CNDs-3 showed an additional peak at 350 nm. This change of the absorption peak is ascribed to the greater variety of amino-functional groups, which caused electron enrichment. The PL emission spectra showed optimal excitation wavelengths of 309, 351, and 379 nm for p-CNDs-1; 302 nm for p-CNDs-2; and 259, 302, and 372 nm for p-CNDs-3. The as-prepared samples showed greatest emission at 448, 445, and 437 nm, respectively. Detailed PL studies with different excitation wavelengths (300−420 nm) showed that the emissions from p-CNDs-1, p-CNDs-2, and p-CNDs-3 were nearly all excitation-independent (Figure 3b,c,f). The absolute PL quantum yields (PLQYs) were calculated to be 16.3%, 26.99%, and 46.83%, respectively (when excited at 370 nm). The FT-IR spectra (Figure 1g) display vibration peaks of hydroxyl, carboxyl, and amide groups; increasing the initial HCl concentration clearly enhanced the C═C, −N−H, and C−N vibrations and gradually weakened the bands assigned to −OH and C−H groups, which indicates a decrease of oxygen-containing functional groups on the carbon skeleton structure and an increase of N-doping. Given that only the synthesis pH differed among the three samples (Figure 1), the pH of the reaction clearly strongly influenced the structures and PLQYs of the three p-CNDs. Furthermore, increasing the HCl concentration altered the color of the samples from bright yellow to deep brown, indicating the beginning of particle nucleation (Figure S1). As a result, HCl appears to benefit the dehydration reaction of the two amino acid molecules, leading to the formation of a carbon core, as shown in Figure 1.

Three paired comparison tests were used to further explore the influence of pH on the synthesis. We changed the molar ratio of the carbon source along with pH, while keeping all other conditions constant. The differing chemical equilibria of p-CNDs-1, p-CNDs-2, and p-CNDs-3 give information about their different structures, and the equilibrium was strongly

DOI: 10.1021/acsami.5b11579
ACS Appl. Mater. Interfaces 2016, 8, 4062−4068

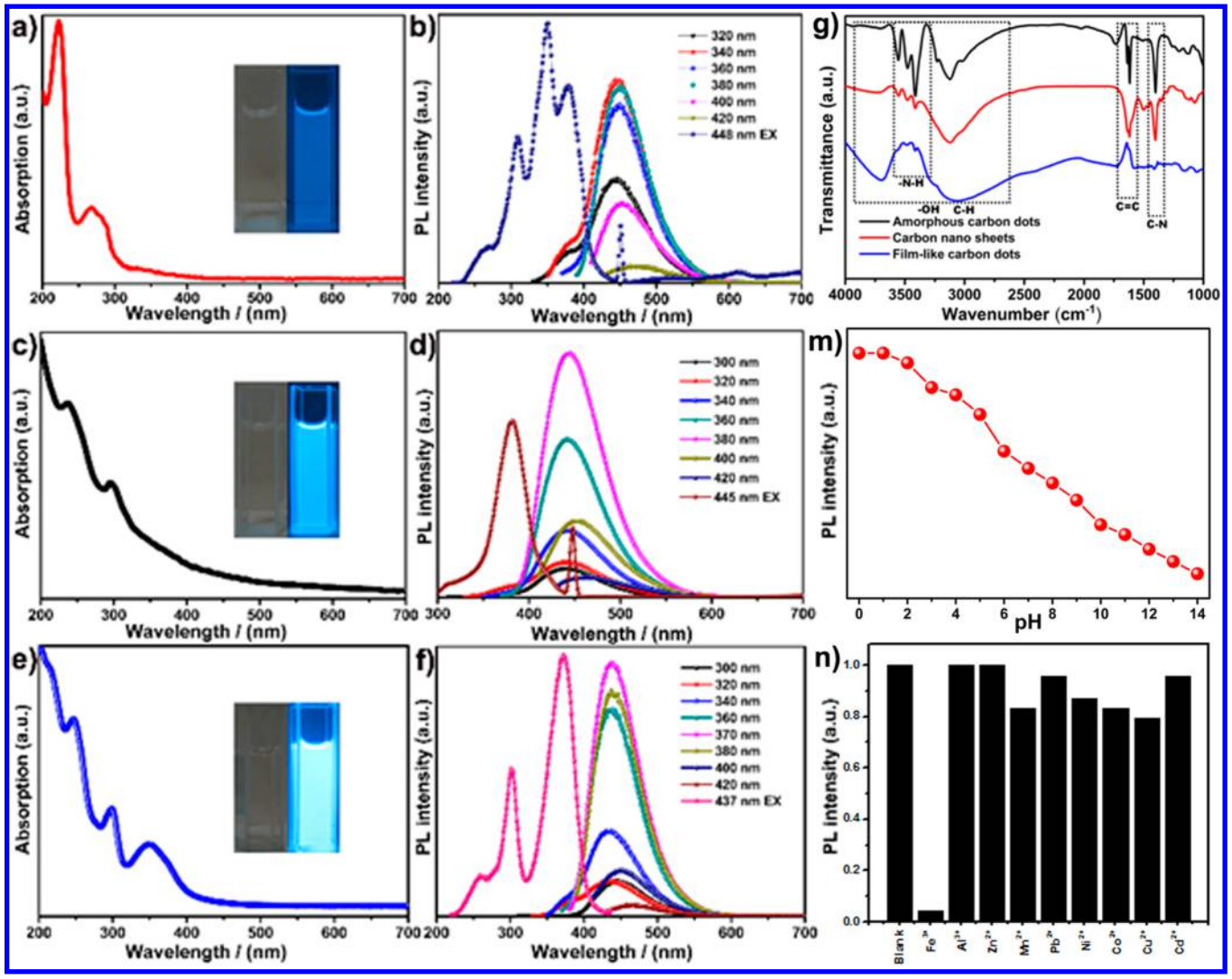

Figure 3. UV−vis absorption and PL spectra of (a, b)film-like carbon dots, (c, d)carbon nano sheets, and (e, f) amorphous carbon dots in aqueous solution at different excitation wavelengths in 20 nm increments starting from 300 to 420 nm. (inset) Photographs of CDs in ethanol solution under a visible light (left) and CDs solution under a UV beam of 365 nm. (g) FT-IR spectra of film-like carbon dots (blue), carbon nanosheets (red), and amorphous carbon dots (black). (m) Relative intensity variation of PL spectra of amorphous carbon dots with the increase of pH value from 1 to 14. (n) The different PL intensities of the amorphous carbon dots solution and the absence of various metal ions.

affected by the initial pH. In a weak basic medium, L-serine and L-tryptophan underwent an amide condensation reaction to form polypeptide chains. Then, the carbon films easily formed via intertwining polypeptide chains and supramolecular weak interactions between the supramolecular polymer. An acidic medium is known to promote the formation of carbon cores, so with decreasing pH, the carbonization degree increased. At 3 < pH < 7, the region that formed films and carbon sheets, many polymer chains remained and linked to the carbon cores. However, at much lower pH, when the sheets gave way to dots, almost all the molecules and polymer chains were further carbonized.

In addition, as shown in Table S1, the PLQY of the as-prepared CNDs from either pure L-serine or pure L-tryptophan were independent of the synthesis pH, while the PLQYs of the CNDs made from a mixture clearly depended on the pH. The PLQYs of the L-serine/L-tryptophan CNDs made in acidic conditions were close to double those of CNDs similarly made in alkaline conditions. The only difference between L-serine and L-tryptophan is the hydroxyl and indolyl groups; therefore, in the acidic medium, the hydroxyl can oxidize L-tryptophan, which was the probable cause of the different reaction paths and the pH dependence of PL.[30]

The pH dependence of the three samples was similar to each other. The PL intensity was highest in strong acid and lowest in strong base (Figure 3m). Moreover, the PL of the three kinds of p-CNDs were all selectively quenched by Fe^{3+} ions (Figure 3n).[31] Therefore, these materials were able to detect H^+ and Fe^{3+} simultaneously.

Synthesis of Super Small Carbon Dots with White Light Emission. CNDs that formed at 300 °C and pH ≈ 0.5 for 16 h (Figure 1) had a narrow size distribution around a mean diameter of 0.5 nm; they self-assembled into SCNDs (Figure 4). Interestingly, the as-synthesized SCNDs exhibited more favorable solubility in ethyl alcohol than in water. More important was their strong white fluorescence, which is rarely observed from CNDs. Previous reports of direct white-light emission include Wang et al.'s synthesis of white-light-emitting CNDs by surface passivation of crude CNDs[32,33] and Chen's CNDs prepared by chemical unzipping.[34] To the best of our

DOI: 10.1021/acsami.5b11579
ACS Appl. Mater. Interfaces 2016, 8, 4062−4068

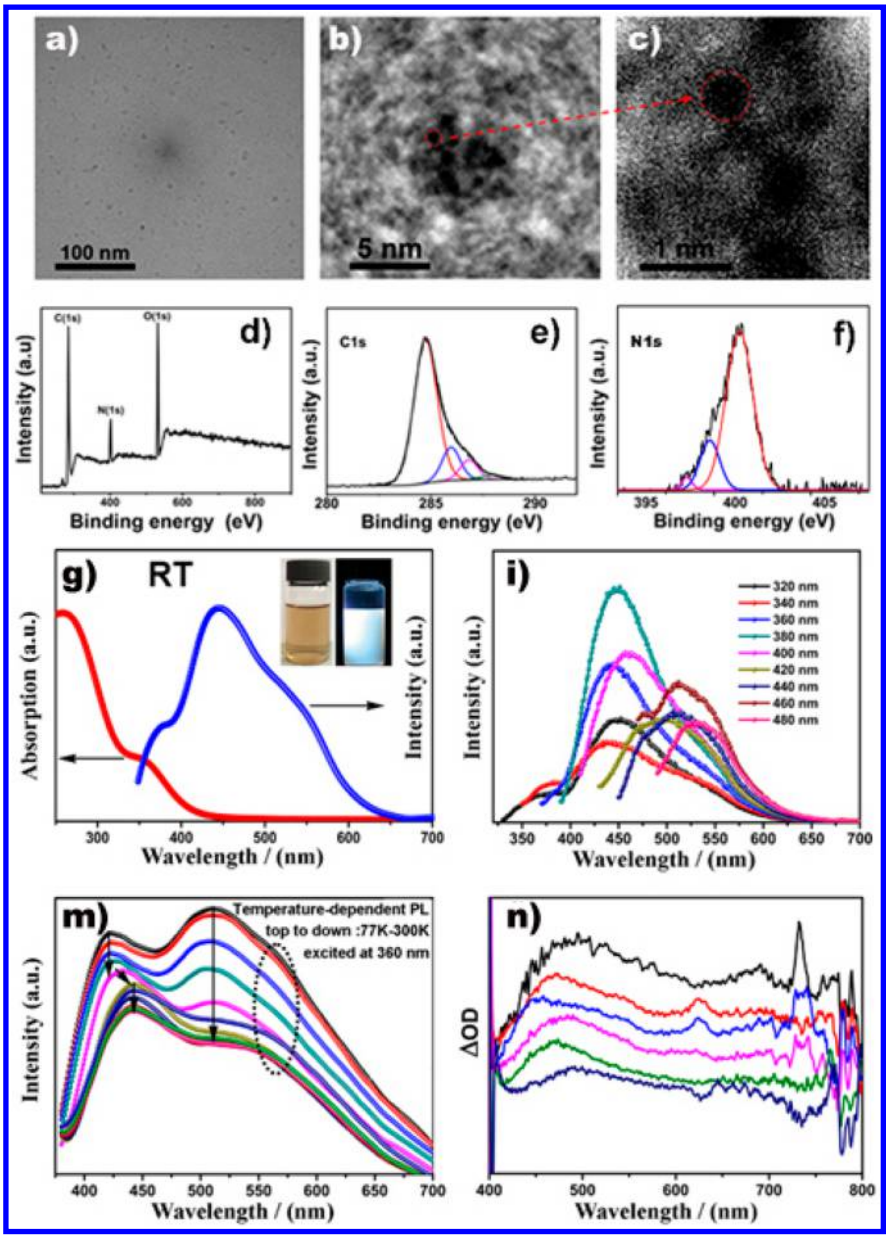

Figure 4. (a) TEM and (b, c) HRTEM images of as-prepared SCNDs. (d, e, f) XPS data for SCNDs. (g) UV−vis absorption spectra and emission spectra of SCNDs (at 320 nm excitation) in ethanol solutions at room temperature. (inset) Photographs of SCNDs in ethanol solution under a visible light (left) and SCDs solution under a UV beam of 365 nm (right). (i) Excitation-dependent PL of SCNDs. (m) Temperature-dependent PL spectra of SCNDs from 77 to 300 K at 360 nm excitation. (n) TA spectra of SCNDs, there was a positive broad excited-state absorption (ESA). 1 ps (black), 4 ps (red), 10 ps (light blue), 100 ps (pink), 660 ps (green), 1300 ps (dark blue).

knowledge, this is the first report of white-emitting CNDs of this small size. Their white emission is visible to the naked eye under irradiation by an ultraviolet lamp (Figure 4g). X-ray photoelectron spectroscopy (XPS) found the SCNDs to comprise mainly carbon, nitrogen, and oxygen (Figure 4d). The high-resolution C 1s spectrum revealed three different types of carbon atom, with the signals at 284.75, 286.1, and 287.1 eV, corresponding to sp^2 or sp^3 carbon,[31] −COOH, and C−N, respectively (Figure 4e). The high-resolution N 1s spectra (Figure 4f) show pyridinic (398.6 eV), pyrrolic (399.7 eV), and graphitic (401.4 eV) N atoms, which confirmed the formation of N-doped SCNDs.

The optical properties of the SCNDs were measured to explore the PL mechanism of their white emission. A broad absorption band appeared at 320 nm in the UV−vis absorption spectrum. The ultrabroad white PL emission band in the visible region (Figure 4g) had a full width at half-maximum (fwhm) of ∼200 nm. The SCNDs in ethanol showed an emission spectrum of chromaticity coordinates (0.36, 0.36) by the standards of the International Commission on Illumination (CIE), 1931 (Figure S3). They also exhibited excitation-dependent emission (Figure 4i). The PL spectra were generally broad, with the fluorescent emission peaks shifting to longer wavelength as the excitation wavelength increased. The absolute PLQYs of the SCNDs was 12.7%, which excited at 360 nm is superior to that reported for many white-light emitters. To explore further the origin of the PL of these particles, temperature-dependent (77−300 K) PL and time-correlated single-photon counting (TCSPC) were performed, which can reveal details of the underlying decay process. The

DOI: 10.1021/acsami.5b11579
ACS Appl. Mater. Interfaces 2016, 8, 4062−4068

temperature-dependent PL employed 360 nm excitation (Figure 4m). At each temperature, the PL spectrum exhibits asymmetric peaks, suggesting multiple fluorophores or diverse surface states. At cryogenic temperatures, the high-energy band has peaks at 420 nm (~3.0 eV) and 512 nm (~2.4 eV). In contrast, the low-energy band has a shoulder peak at 566 nm (~2.2 eV). The figure shows that with increasing temperature the intensity of fluorescence monotonically decreased, with the strong peak at 512 nm almost completely disappearing, the 423 nm peak becoming red-shifted, and the 566 nm peak remaining nearly stable. The loss of emission might be attributable to the surface-state carbon dots. Despite ions or solvent attachment inducing emissive traps on the surface of the CNDs, only the surface-state emission was highly susceptible to environment changes, while the intrinsic emission was not. Heating led radiative relaxation in the SCNDs to have an increasing effect, sharply decreasing the intensity.[35,36] Notably, heating from 160 to 200 K caused strong (21 nm) red shifting from 420 to 441 nm, which was attributed to the ethanol phase transition. In this interacting environment, an additional relaxation step (solvation) occurred in the fluorescence process. After excitation, the fluorophore and the ethanol dipole were no longer in equilibrium. The liquid ethanol dipole could rotate to align with the excited fluorophore, reducing its interaction energy and thus lowering the energy of the excited fluorophore. Therefore, the net result of solvent relaxation was to red-shift the fluorescence. Figure S4 shows long PL lifetimes over the whole emission spectra of the SCNDs, and the PL lifetimes of the SCNDs were on the order of nanoseconds. This indicates that only the SCNDs had fluorescent properties.

The origin of the PL of the SCNDs was further investigated by femtosecond broad-band (350−800 nm) transient absorption (TA) spectroscopy at 400 nm excitation (Figure 4n). A TA spectrum usually shows three kinds of spectral features. After the pump light excitation, the Pauli exclusion principle causes the filling of quantum electronic states to lead to the bleaching of the corresponding optical transitions from the ground state to the excited state; this is ground-state bleaching (GSB). In contrast, the photoexcited electrons in the excited states either absorb probe light at higher levels or return to the ground state by stimulated radiation due to the disturbance by the probe light, which is either excited-state absorption (ESA) or stimulated emission, respectively. All the features of a TA spectrum reflect information about the change of photogenerated carrier populations in the corresponding energy levels. The SCNDs showed positive, broad, excited-state absorption, indicating that they contained a multilevel, highly emissive recombination channel, which could possibly have arisen from the wide distributions of surface-state PL centers.

The PL mechanism was further explored through a series of N-doped polyaromatic structures produced to model the N-doping within the carbon dots' structure. Polyaromatic structures with seven aromatic cycles and N atoms substituted at different positions were constructed and optimized. All the calculations used the Gaussian09 package. The optimized geometries required for calculation in the gas phase were obtained from density functional theory at the B3LYP/6-31++G(d,p) level.[37] The resulting band gaps are displayed in Figures 5 and S5. The fluorescence of the differently N-doped CNDs extended across the entire visible region.

Supersmall Carbon Dots for White Light-Emitting Diodes. Direct white-light emitters have attracted much recent interest for their application in the development of solid-state lighting.[38,39] Direct light generation is photoluminescent from only one type of nanocrystal layer, and devices employing such white-light emission can be excited by UV LEDs. We designed hybrid nanocomposites by polymerizing SCNDs in a *N*,*N*-dimethylacetoacetamide (DMAA) solution. The blended DMAA and SCNDs compounds (DMAA/SCNDs) also exhibited white-light emission and excitation-dependent emissions (Figure S6), which resulted from the SCNDs' emissions within the sample. The as-polymerized DMAA/SCNDs easily formed a monolith (Figure 6d), which upon excitation with a UV lamp (Figure 6e−g) exhibited bright white emission at extreme temperatures (Figure S6). They remained emissive for over 14 months under ambient conditions. No dramatic photobleaching was then found after 12 h of continuous UV exposure (Figure S6), which is significant, because it is a necessary property for their application in LEDs. The monoliths are superior to other dye or semiconductor quantum dots embedded in films or glass in terms of their ease of fabrication, high photostability, complete homogeneity, and low toxicity, all of which suggest that the SCNDs have great potential to become a new class of phosphor material for emerging color-emitting technologies such as LEDs based on UV chips. We directly employed the as-prepared solid DMAA/SCNDs compounds as phosphors to construct LEDs. The devices were made by coating DMAA/SCNDs on a prototype solid-state lighting unit comprising an excitation (365 nm) light-emitting chip and then subsequently in situ polymerizing them. The resulting emission spectra (Figure 6b) show two components: one from the chip centered at 365 nm and the corresponding visible component in the range of 410−700 nm from the SCNDs. We also analyzed the emission spectra of the SCNDs in the LED devices for their color emission. The CIE coordinates of (0.29, 0.31) show that these SCNDs are useful as a single white-light phosphor for a white LED. In addition, the CRI and CCT are 81 and 6786 K, respectively. This represents a significant advancement in the applicability of CNDs.

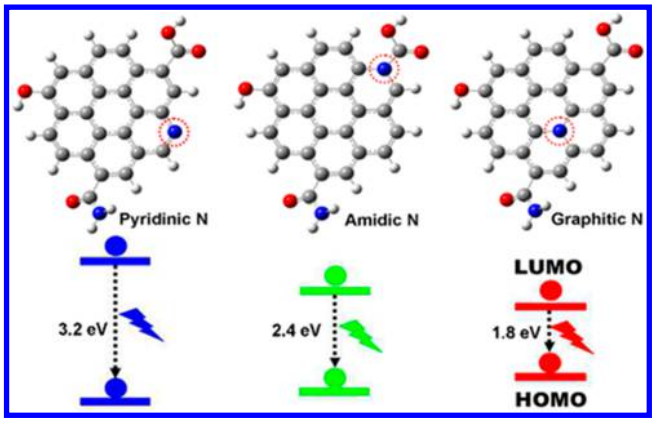

Figure 5. Optimized structures of different positions nitrogen doped in carbon skeleton and scheme of white-light-emission SCNDs.

CONCLUSION

In summary, pH-controlled morphology of CNDs's were obtained. Their chemical structure and PL mechanism were investigated in detail. Cross-linked polymer film, carbon nanosheets, and amorphous carbon dots were achieved by altering the synthesis pH values. More importantly, by increasing synthesis temperature, we obtained the SCNDs,

DOI: 10.1021/acsami.5b11579
ACS Appl. Mater. Interfaces 2016, 8, 4062−4068

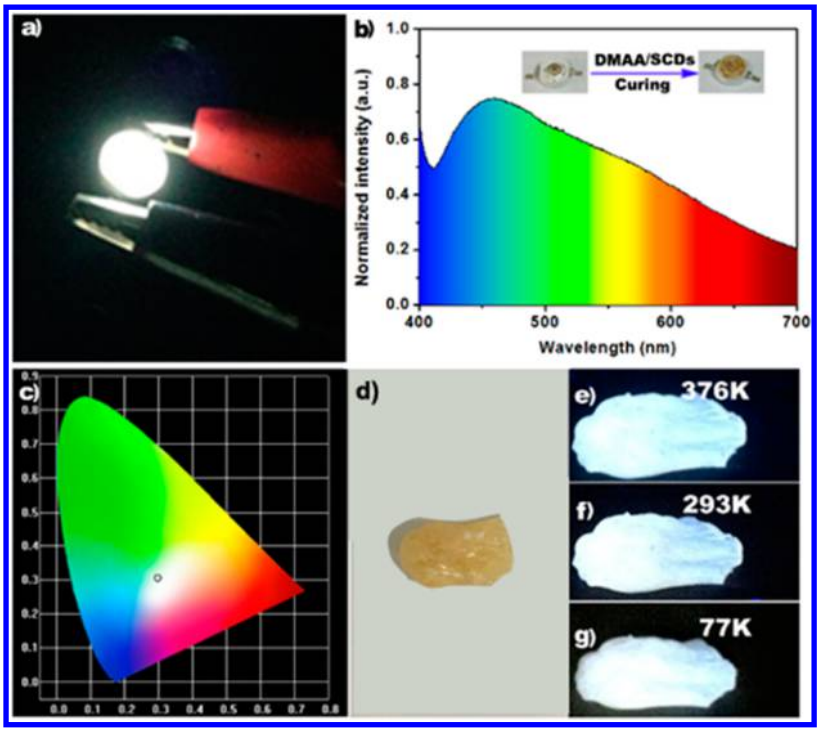

Figure 6. (a) WLEDs images of as-prepared DMAA/SCNDs. (b) Emission spectra of WLEDs. (c) Placement of the SCNDs emission spectra on the CIE 1931 chromaticity chart (0.29, 0.31). (d) The bulk DMAA/SCNDs material under a visible light. (e–g) UV beam of 365 nm at different temperature.

which were the real white emission and easily applied as inexpensive in WLEDs. The relationship between the structure and the corresponding fluorescence was thoroughly investigated, and we suggest a mechanism of the PL of the CNDs. Understanding their PL mechanism might aid investigations of the PL mechanisms of other carbon-based fluorescent materials.

■ ASSOCIATED CONTENT

Supporting Information

The Supporting Information is available free of charge on the ACS Publications website at DOI: 10.1021/acsami.5b11579.

Preparations of carbon dot, DMAA/SCNDs, and WLEDs from SCNDs, FT-IR spectra, photograph of original p-SCNDs at different HCl concentration, the time-correlated single-photon counting of SCNDs, PL data for super carbon dots in DMAA, the stability of bulk DMAA/SCNDs material, and the calculated band gaps of different N doping site in carbon skeleton. (PDF)

■ AUTHOR INFORMATION

Corresponding Author

*E-mail: byangchem@jlu.edu.cn. Fax: +86 431 85193423.

Notes

The authors declare no competing financial interest.

■ ACKNOWLEDGMENTS

This work was supported by the National Science Foundation of China (51373065, 91123031, and 21221063), the National Basic Research Program of China (2012CB933800), and Specialized Research Fund for the Doctoral Program of Higher Education (20130061130010)

■ REFERENCES

(1) Li, H.; Kang, Z.; Liu, Y.; Lee, S. T. Carbon nanodots: Synthesis, Properties and Applications. *J. Mater. Chem.* **2012**, *22*, 24230.
(2) Lou, Q.; Qu, S.; Jing, P.; Ji, W.; Li, D.; Cao, J.; Zhang, H.; Liu, L.; Zhao, J.; Shen, D. Water-Triggered Luminescent "Nano-bombs" Based on Supra-(Carbon Nanodots). *Adv. Mater.* **2015**, *27*, 1389–1394.
(3) Bhunia, S. K.; Saha, A.; Maity, A. R.; Ray, S. C.; Jana, N. R. Carbon Nanoparticle-based Fluorescent Bioimaging Probes. *Sci. Rep.* **2013**, *3*, 1473.
(4) Baker, S. N.; Baker, G. A. Luminescent Carbon Nanodots: Emergent Nanolights. *Angew. Chem., Int. Ed.* **2010**, *49*, 6726–6744.
(5) Wu, Z. Y.; Li, C.; Liang, H. W.; Chen, J. F.; Yu, S. H. Ultralight, Flexible, and Fire-Resistant Carbon Nanofiber Aerogels from Bacterial Cellulose. *Angew. Chem., Int. Ed.* **2013**, *52*, 2925–2929.
(6) Wang, L.; Zhu, S. J.; Wang, H. Y.; Qu, S. N.; Zhang, Y. L.; Zhang, J. H.; Chen, Q. D.; Xu, H. L.; Han, W.; Yang, B.; Sun, H. B. Common Origin of Green Luminescence in Carbon Nanodots and Graphene Quantum Dots. *ACS Nano* **2014**, *8*, 2541–2547.
(7) Krysmann, M. J.; Kelarakis, A.; Dallas, P.; Giannelis, E. P. Formation Mechanism of Carbogenic Nanoparticles with Dual Photoluminescence Emission. *J. Am. Chem. Soc.* **2012**, *134*, 747–750.
(8) Tang, L.; Ji, R.; Cao, X.; Lin, J.; Jiang, H.; Li, X.; Teng, K. S.; Luk, C. M.; Zeng, S.; Hao, J.; Lau, S. P. Deep Ultraviolet Photoluminescence of Water-Soluble Self-Passivated Graphene Quantum Dots. *ACS Nano* **2012**, *6*, 5102–5110.
(9) Lingam, K.; Podila, R.; Qian, H.; Serkiz, S.; Rao, A. M. Evidence for Edge-State Photoluminescence in Graphene Quantum Dots. *Adv. Funct. Mater.* **2013**, *23*, 5062–5065.
(10) Zhu, S.; Zhang, J.; Wang, L.; Song, Y.; Zhang, G.; Wang, H.; Yang, B. A General Route to Make Non-Conjugated Linear Polymers Luminescent. *Chem. Commun.* **2012**, *48*, 10889–10891.
(11) Pan, D.; Zhang, J.; Li, Z.; Wu, M. Hydrothermal Route for Cutting Graphene Sheets into Blue-Luminescent Graphene Quantum Dots. *Adv. Mater.* **2010**, *22*, 734–738.
(12) Chen, Z. L.; Zhang, H.; Yu, W.; Li, Z.; Hou, J.; Wei, H.; Yang, B. Inverted Hybrid Solar Cells from Aqueous Materials with a PCE of 3.61%. *Adv. Energy. Mater.* **2013**, *3*, 433–437.

DOI: 10.1021/acsami.5b11579
ACS Appl. Mater. Interfaces 2016, 8, 4062–4068

(13) Zhu, S.; Meng, Q.; Wang, L.; Zhang, J.; Song, Y.; Jin, H.; Zhang, K.; Sun, H.; Wang, H.; Yang, B. Highly Photoluminescent Carbon Dots for Multicolor Patterning, Sensors, and Bioimaging. *Angew. Chem., Int. Ed.* **2013**, *52*, 3953−3957.
(14) Xu, X.; Ray, R.; Gu, Y.; Ploehn, H. J.; Gearheart, L.; Raker, K.; Scrivens, W. A. Electrophoretic Analysis and Purification of Fluorescent Single-Walled Carbon Nanotube Fragments. *J. Am. Chem. Soc.* **2004**, *126*, 12736−12737.
(15) Sun, Y. P.; Zhou, B.; Lin, Y.; Wang, W.; Fernando, K. A.; Pathak, P.; Meziani, M. J.; Harruff, B. A.; Wang, X.; Wang, H.; Luo, P. G.; Yang, H.; Kose, M. E.; Chen, B.; Veca, L. M.; Xie, S. Y. Quantum-Sized Carbon Dots for Bright and Colorful Photoluminescence. *J. Am. Chem. Soc.* **2006**, *128*, 7756−7757.
(16) Sun, Y.; Cao, W.; Li, S.; Jin, S.; Hu, K.; Hu, L.; Huang, Y.; Gao, X.; Wu, Y.; Liang, X. J. Ultrabright and Multicolorful Fluorescence of Amphiphilic Polyethyleneimine Polymer Dots for Efficiently Combined Imaging and Therapy. *Sci. Rep.* **2013**, *3*, 3036.
(17) Li, Y.; Hu, Y.; Zhao, Y.; Shi, G.; Deng, L.; Hou, Y.; Qu, L. An Electrochemical Avenue to Green-Luminescent Graphene Quantum Dots as Potential Electron-Acceptors for photovoltaics. *Adv. Mater.* **2011**, *23*, 776−780.
(18) Bourlinos, A. B.; Stassinopoulos, A.; Anglos, D.; Zboril, R.; Georgakilas, V.; Giannelis, E. P. Photoluminescent Carbogenic Dots. *Chem. Mater.* **2008**, *20*, 4539−4541.
(19) Loh, K. P.; Bao, Q.; Eda, G.; Chhowalla, M. Graphene Oxide as a Chemically Tunable Platform for Optical Applications. *Nat. Chem.* **2010**, *2*, 1015−1024.
(20) Zhu, S.; Zhang, J.; Tang, S.; Qiao, C.; Wang, L.; Wang, H.; Liu, X.; Li, B.; Li, Y.; Yu, W.; Wang, X.; Sun, H.; Yang, B. Surface Chemistry Routes to Modulate the Photoluminescence of Graphene Quantum Dots: From Fluorescence Mechanism to Up-Conversion Bioimaging Applications. *Adv. Funct. Mater.* **2012**, *22*, 4732−4740.
(21) Li, H.; He, X.; Kang, Z.; Huang, H.; Liu, Y.; Liu, J.; Lian, S.; Tsang, C. H.; Yang, X.; Lee, S. T. Water-Soluble Fluorescent Carbon Quantum Dots and Photocatalyst Design. *Angew. Chem., Int. Ed.* **2010**, *49*, 4430−4434.
(22) Liu, J.; Liu, Y.; Liu, N. Y.; Han, Y. Z.; Zhang, X.; Huang, H.; Lifshitz, Y.; Lee, S. T.; Zhong, J.; Kang, Z. H. Metal-Free Efficient Photocatalyst For Stable Visible Water Splitting via a Two-Electron Pathway. *Science* **2015**, *347*, 970−974.
(23) Das, S. K.; Liu, Y.; Yeom, S.; Kim, D. Y.; Richards, C. I. Single-Particle Fluorescence Intensity Fluctuations of Carbon Nanodots. *Nano Lett.* **2014**, *14*, 620−625.
(24) Zhu, S.; Zhang, J.; Qiao, C.; Tang, S.; Li, Y.; Yuan, W.; Li, B.; Tian, L.; Liu, F.; Hu, R.; Gao, H.; Wei, H.; Zhang, H.; Sun, H.; Yang, B. Strongly Green-Photoluminescent Graphene Quantum Dots for Bioimaging Applications. *Chem. Commun.* **2011**, *47*, 6858−6860.
(25) Ye, R.; Xiang, C.; Lin, J.; Peng, Z.; Huang, K.; Yan, Z.; Cook, N. P.; Samuel, E. L.; Hwang, C. C.; Ruan, G.; Ceriotti, G.; Raji, A. R.; Marti, A. A.; Tour, J. M. Coal as an Abundant Source of Graphene Quantum Dots. *Nat. Commun.* **2013**, *4*, 2943.
(26) Brown, A. L.; Goforth, A. M. pH-Dependent Synthesis and Stability of Aqueous, Elemental Bismuth Glyconanoparticle Colloids: Potentially Biocompatible X-ray Contrast Agents. *Chem. Mater.* **2012**, *24*, 1599−1605.
(27) Wu, S. T.; Long, L. S.; Huang, R. B.; Zheng, L. S. pH-Dependent Assembly of Supramolecular Architectures from 0D to 2D Networks. *Cryst. Growth Des.* **2007**, *7*, 1747.
(28) Liu, C.; Luo, F.; Liao, W. P.; Li, D. Q.; Wang, X. F.; Dronskowski, R. pH-Dependent Syntheses and Structures of Two Copper(II)/Phenanthroline/p-Sulfonatocalix[4]arene Supramolecular Compounds with 1D Water-Filled Channels. *Cryst. Growth Des.* **2007**, *7*, 2283.
(29) Lu, S. Y.; Zhu, S. J.; Yang, B.; Zhao, X.; Song, Y. Novel Cookie-with-chocolate Carbon Dots Displaying Extremely Acidophilic Luminescence. *Nanoscale* **2014**, *6*, 13939.
(30) Casbeer, E. M.; Sharma, V. K.; Zajickova, Z.; Dionysiou, D. D. Kinetics and Mechanism of Oxidation of Tryptophan by Ferrate (VI). *Environ. Sci. Technol.* **2013**, *47*, 4572−4580.
(31) Song, Y.; Zhu, S.; Xiang, S.; Zhao, X.; Zhang, J.; Zhang, H.; Fu, Y.; Yang, B. Investigation into the Fluorescence Quenching Behaviors and Applications of Carbon Dots. *Nanoscale* **2014**, *6*, 4676−4682.
(32) Wang, F.; Chen, Y. H.; Liu, C. Y.; Ma, D. G. White Light-Emitting Devices Based on Carbon Dots' Electroluminescence. *Chem. Commun.* **2011**, *47*, 3502−3504.
(33) Wang, F.; Kreiter, M.; He, B.; Pang, S.; Liu, C. Synthesis of Direct White-Light Emitting Carbogenic Quantum dots. *Chem. Commun.* **2010**, *46*, 3309−3311.
(34) Guo, X.; Wang, C. F.; Yu, Z. Y.; Chen, L.; Chen, S. Facile Access to Versatile Fluorescent Carbon Dots toward Light-Emitting Diodes. *Chem. Commun.* **2012**, *48*, 2692−2694.
(35) Li, X. M.; Liu, Y. L.; Zeng, H. B.; Song, X.; Wang, H.; Gu, H. Intercrossed Carbon Nanorings with Pure Surface States as Low-Cost and Environment-Friendly Phosphors for White-Light-Emitting Diodes. *Angew. Chem., Int. Ed.* **2015**, *54*, 1759−1764.
(36) Yu, P.; Wen, X.; Toh, Y.-R.; Tang, J. Temperature-Dependent Fluorescence in Carbon Dots. *J. Phys. Chem. C* **2012**, *116*, 25552−25557.
(37) Frisch, M. J.; Trucks, G. W.; Schlegel, H. B.; Scuseria, G. E.; Robb, M. A.; Cheeseman, J. R.; Scalmani, G.; Barone, V.; Mennucci, B.; Petersson, G. A.; Nakatsuji, H.; Caricato, M.; Li, X.; Hratchian, H. P.; Izmaylov, A. F.; Bloino, J.; Zheng, G.; Sonnenberg, J. L.; Hada, M.; Ehara, M.; Toyota, K.; Fukuda, R.; Hasegawa, J.; Ishida, M.; Nakajima, T.; Honda, Y.; Kitao, O.; Nakai, H.; Vreven, T.; Montgomery, J. A. Jr.; Peralta, J. E.; Ogliaro, F.; Bearpark, M.; Heyd, J. J.; Brothers, E.; Kudin, K. N.; Staroverov, V. N.; Kobayashi, R.; Normand, J.; Raghavachari, K.; Rendell, A.; Burant, J. C.; Iyengar, S. S.; Tomasi, J.; Cossi, M.; Rega, N.; Millam, N. J.; Klene, M.; Knox, J. E.; Cross, J. B.; Bakken, V.; Adamo, C.; Jaramillo, J.; Gomperts, R.; Stratmann, R. E.; Yazyev, O.; Austin, A. J.; Cammi, R.; Pomelli, C.; Ochterski, J. W.; Martin, R. L.; Morokuma, K.; Zakrzewski, V. G.; Voth, G. A.; Salvador, P.; Dannenberg, J. J.; Dapprich, S.; Daniels, A. D.; Farkas, Ö.; Foresman, J. B.; Ortiz, J. V.; Cioslowski, J.; Fox, D. J. *Gaussian 09*, Gaussian, Inc: Wallingford, CT, 2009.
(38) Zhang, X. J.; Huang, L.; Pan, F. J.; Wu, M. M.; Wang, J.; Chen, Y.; Su, Q. Highly Thermally Stable Single-Component White-Emitting Silicate Glass for Organic-Resin-Free White-Light-Emitting Diodes. *ACS Appl. Mater. Interfaces* **2014**, *6*, 2709−2717.
(39) Zhang, X. J.; Yu, J. B.; Wang, J.; Zhu, C. B.; Zhang, J. H.; Zou, R.; Lei, B. F.; Liu, Y. L.; Wu, M. M. Facile Preparation and Ultrastable Performance of SingleComponent White-Light-Emitting Phosphor-in-Glass used for HighPower Warm White LEDs. *ACS Appl. Mater. Interfaces* **2015**, *7*, 28122−28127.

DOI: 10.1021/acsami.5b11579
ACS Appl. Mater. Interfaces 2016, 8, 4062−4068